One-dimensional solidification of an alloy with a mushy zone: thermodiffusion and temperature-dependent diffusivity

By D. V. ALEXANDROV and D. L. ASEEV

Department of Mathematical Physics, Urals State University, Lenin ave. 51,
Ekaterinburg, 620083, Russia
Dmitri.Alexandrov@usu.ru

The effect of a temperature-dependent solute diffusion coefficient on a model of uni-directional solidification of a binary melt with a quasi-equilibrium mushy (two-phase) zone is studied. The Soret effect (thermodiffusion) is also included in the analysis. The concentration field in the liquid, solid and mushy phases, as well as the rate of solidification and mushy zone thickness, are found analytically as functions of all thermophysical parameters. The role of the nonlinear solute transport is detailed in the analysis. On the basis of analytical solutions, the regime of solidification with a quasi-equilibrium mushy zone is replaced by an equivalent discontinuity surface (frontal) regime with new boundary conditions.

1. Introduction

Solidification processes play a very important role in metallurgy and in many cases completely determine the physical and mechanical properties of solid alloys. Sometimes, it is possible to describe crystallization in a standard way by means of the well-known Stefan thermodiffusion model with a planar front (the boundary of phase transition). However, often the plane front of solidification is broken by the constitutional supercooling arising under certain circumstances ahead of the front (Ivantsov 1951). For this reason, some parts of the front grow in more favourable conditions than others, i.e. the front becomes morphologically unstable (Mullins & Sekerka 1964). The evolution of such an instability leads to the appearance of a metastable zone between solid and liquid phases, which is called the two-phase zone or mushy region. Thus, after a lapse of time, solidification is divided into three parts: solid, mushy and liquid phases. A theoretical description of such a scenario of binary melt crystallization was suggested by Hills, Loper & Roberts (1983), Fowler (1985) and Borisov (1987). At present, this nonlinear model is solved for different cases without considering the Soret effect and temperature-dependent diffusion. Attempts at obtaining approximate solutions were made by a number of investigators (Hills *et al.* 1983; Fowler 1985; Worster 1986; Borisov 1987; Buyevich, Alexandrov & Mansurov 2001). However, exact analytical solutions were obtained by Alexandrov (2001), who analysed the solidification of a binary melt with a mushy region, in which heterogeneous inclusions of the new phase grow in such a manner that this region is almost totally desupercooled. We shall consider this model but include also the Soret effect and temperature-dependent diffusion. Huppert & Worster (1985) outline six different regimes that arise depending on whether the initial liquid concentration

is less than, equal to, or greater than the eutectic composition, and whether the liquid is cooled from an upper or a lower horizontal boundary. Following the model by Worster (1986), we shall investigate solidification in the absence of gravity, though this situation may almost be realized in the laboratory (Huppert & Worster 1985) by cooling, from below, a liquid whose initial concentration is less than the eutectic value, since then the temperature and concentration fields are individually statically stable to convective turnover.

The diffusion flux determines the solute gradient in the liquid at a given growth rate and, consequently, determines the value of the constitutional supercooling. However, since the liquid temperature gradient is often high, thermodiffusion (Soret effect) should be considered as well. In many cases, thermodiffusion may have a strong dependence on composition. In particular, for dilute solutions, the thermodiffusion flux is proportional to the mean concentration (see, for example, Van Vaerenbergh *et al.* 1998). Our interest here is therefore be analyse a dependence diffusion flux of the form:

$$\boldsymbol{J} = -D\boldsymbol{\nabla}\sigma - D_T(\beta_0 + \beta_1\sigma)\boldsymbol{\nabla}\theta, \tag{1}$$

where σ and θ are the concentration and temperature fields, D is the diffusion coefficient, D_T is the thermodiffusion coefficient and β_0 and β_1 are constants. We are primary interested in two cases, namely Model I for which $\beta_0 = \sigma_\infty$, where σ_∞ is the initial concentration and $\beta_1 = 0$, and Model II for which $\beta_0 = 0$ and $\beta_1 = 1$. The first case, discussed by Van Vaerenbergh *et al.* (1995), corresponds to small variations in the concentration field. However, for dilute solutions and for all cases where the transport is of thermophoretic form (each particle of solute being driving by a thermal 'force' without interaction between them) and so may exhibit unusual dynamics, Model II is more correct (Van Vaerenbergh, Coriell & McFadden 2001).

The Dufour effect, where concentration gradients change temperature, reciprocal to the Soret effect where temperature gradients change concentration, is also known from irreversible thermodynamics. However, in binary liquid mixtures the Dufour effect is negligible (this effect is most important in gas mixtures; see, among others, Hollinger & Lücke 1995).

Generally speaking, the diffusion coefficient is not a constant with temperature. Let us write this function in a linear form (Bruson & Gerl 1980; Van Vaerenbergh *et al.* 2001):

$$D(\theta) = D_0 + \frac{\partial D}{\partial \theta}(\theta - \theta_0), \tag{2}$$

where D_0 is the diffusion coefficient at the melting temperature θ_0 and $\partial D/\partial \theta$ is the temperature coefficient. Our theory is devoted to exact analytical solutions of the solidification with a mushy zone on the basis of nonlinear solute transport (1), (2).

2. The model

Let us consider a unidirectional process of binary melt solidification along axis ξ (the constant rate u_s of solidification and the mushy zone thickness δ will be regarded as established). In other words, solidification proceeds far from the walls of an ingot mould and their influence on the process is not significant. Therefore, it is reasonable to assume that temperature gradients in the solid g_s and liquid g_l phases are fixed.

The regions $\xi < u_s\tau$ and $\xi > u_s\tau + \delta$ are filled with the solid and liquid (melt) phases, respectively, and the mushy zone is placed between boundaries $\xi = u_s\tau$ and

$\xi = u_s\tau + \delta$. The projection of the diffusion flux (1) on the direction ξ is

$$J = -D_m(\theta)\frac{\partial\sigma}{\partial\xi} - D_{Tm}(\beta_0 + \beta_1\sigma)\frac{\partial\theta}{\partial\xi}.$$

Here D_m and D_{Tm} are the diffusion and thermodiffusion coefficients in the mushy zone. A set of equations describing heat and mass transfer in the mushy zone and adjoining phases has the form

$$\frac{\partial}{\partial\tau}[(1-\varphi)\sigma] = -\frac{\partial}{\partial\xi}J - k\sigma\frac{\partial\varphi}{\partial\tau}, \quad u_s\tau < \xi < u_s\tau + \delta, \tag{3}$$

$$\frac{\partial}{\partial\tau}[\rho C\theta] = \frac{\partial}{\partial\xi}\left(\lambda\frac{\partial\theta}{\partial\xi}\right) + L_V\frac{\partial\varphi}{\partial\tau}, \quad u_s\tau < \xi < u_s\tau + \delta, \tag{4}$$

$$\theta = \theta_0 - m\sigma, \quad u_s\tau < \xi < u_s\tau + \delta, \tag{5}$$

$$\frac{\partial\sigma_l}{\partial\tau} = -\frac{\partial}{\partial\xi}J_l, \quad J_l = -D(\theta_l)\frac{\partial\sigma_l}{\partial\xi} - D_T(\beta_0 + \beta_1\sigma_l)\frac{\partial\theta_l}{\partial\xi}, \quad \xi > u_s\tau + \delta,$$

$$\frac{\partial\theta_l}{\partial\xi} = g_l, \quad \xi > u_s\tau + \delta, \quad \frac{\partial\theta_s}{\partial\xi} = g_s, \quad \xi < u_s\tau. \tag{6}$$

Here σ and σ_l are the concentrations of impurity in the mushy and liquid phases (neglecting diffusion in the solid), θ, θ_l and θ_s are the temperatures in the mushy, melt and solid phases, φ is the bulk fraction of the solid phase in the mush, D and D_T are the diffusion and thermodiffusion coefficients in the liquid, m is the liquidus slope determined from the phase diagram, k is the equilibrium partition coefficient, ρ is the density, C is the thermal capacity, λ is the thermal conductivity and L_V is the latent heat of solidification per unit mass.

We assume that the molecular transport processes are given by volume-fraction-weighted averages

$$\lambda = \lambda_l(1-\varphi) + \lambda_s\varphi, \quad D_m = D(1-\varphi), \quad D_{Tm} = D_T(1-\varphi), \tag{7}$$

having ignored chemical diffusion in the solid phase (λ_l and λ_s are the thermal conductivities in the liquid and solid phases). These expressions are only approximate, since such transport coefficients should generally depend upon the internal morphology of the two-phase medium (Batchelor 1974), but these expression have been found to lead to good agreement with the results of laboratory experiments on stagnant mushy layers (Huppert & Worster 1985; Worster 1986; Kerr *et al.* 1990*a, b, c*). We emphasize that the linear form of the function $\lambda = \lambda(\varphi)$ is not essential for the theory under consideration. We use only the continuity expression $\lambda|_{\xi=u_s\tau+\delta} = \lambda_l$.

Further, we neglect the left-hand side of equation (4), because the relaxation time $\tau_a = l^2/a$ of temperature fields is essentially less then the relaxation time $\tau_D = l^2/D_l$ of the diffusion field, i.e. $\tau_a/\tau_D \sim 10^{-3}-10^{-4}$ (l is a characteristic length scale, and a is the temperature diffusivity coefficient).

We also suppose that the impurity concentration in the melt far from the mush/liquid boundary is known:

$$\sigma_l \longrightarrow \sigma_\infty, \quad \xi \longrightarrow \infty. \tag{8}$$

The following conditions imposed at the boundaries $u_s\tau$ and $u_s\tau + \delta$ hold:

$$\lambda_s g_s - \lambda\frac{\partial\theta}{\partial\xi} = L_V(1-\varphi)u_s, \quad (1-k)(1-\varphi)\sigma u_s = J, \quad \xi = u_s\tau, \tag{9}$$

$$\lambda \frac{\partial \theta}{\partial \xi} = \lambda_l g_l, \quad \varphi = 0, \quad \sigma = \sigma_l, \quad J = J_l, \quad \xi = u_s \tau + \delta, \tag{10}$$

$$\theta = \theta_s, \quad \xi = u_s \tau, \quad \theta = \theta_l, \quad \xi = u_s \tau + \delta. \tag{11}$$

The value of $\varphi_* = \varphi|_{\xi = u_s \tau}$ is not a given parameter.

The next section is concerned with analytical solutions of the model (1)–(11) describing thermodiffusion and temperature-dependent diffusivity in the liquid phase during directional solidification of a dilute binary alloy.

3. Exact analytical solutions

We use the frame of reference associated with the solid/mush interface ($y = \xi - u_s \tau$). In this case, the solidification process is stationary. Let us introduce the following dimensionless variables and parameters:

$$x = \frac{u_s}{D_0} y = \frac{u_s}{D_0}(\xi - u_s \tau), \quad c = \frac{\sigma}{\sigma_\infty}, \quad c_l = \frac{\sigma_l}{\sigma_\infty}, \quad N = \frac{\lambda_s m \sigma_\infty}{L_V D_0},$$

$$\Lambda(\varphi) = \frac{\lambda(\varphi)}{\lambda_s}, \quad \varepsilon = \frac{\delta u_s}{D_0}, \quad G_s = \frac{g_s D_0}{m \sigma_\infty u_s}, \quad G_l = \frac{g_l D_0}{m \sigma_\infty u_s},$$

where x, c and ε are the dimensionless spatial coordinate, solute concentration and mushy zone thickness, respectively. Equation (5) implies that $\partial \theta / \partial \xi = -m \partial \sigma / \partial \xi$ throughout the mushy zone. Taking this into account, let us write equations (3) and (4) supplemented by boundary conditions (9) and (10) in dimensionless form:

$$\frac{d}{dx}\left[(1 - \varphi)c + (1 - \varphi)(a - bc)\frac{dc}{dx}\right] + kc\frac{d\varphi}{dx} = 0, \quad 0 < x < \varepsilon, \tag{12}$$

$$N\frac{d}{dx}\left[\Lambda(\varphi)\frac{dc}{dx}\right] + \frac{d\varphi}{dx} = 0, \quad 0 < x < \varepsilon, \tag{13}$$

$$G_s + \Lambda(\varphi_*)\frac{dc}{dx} = \frac{1 - \varphi_*}{N}, \quad (1 - k)c = -(a - bc)\frac{dc}{dx}, \quad x = 0, \tag{14}$$

$$G_l + \frac{dc}{dx} = 0, \quad c = c_l, \quad \frac{dc}{dx} = \frac{dc_l}{dx}, \quad x = \varepsilon, \tag{15}$$

where $a = 1 - m\beta_0 D_T / D_0$ and $b = (\partial D / \partial \theta + \beta_1 D_T)m\sigma_\infty / D_0$.

Taking into account boundary conditions (8)–(11), solutions of equations (6) can be written as

$$\left.\begin{array}{l} \theta_s = \theta_0 - m\sigma_\infty c|_{x=0} + \dfrac{D_0}{u_s} g_s x, \quad \theta_l = \theta_0 - m\sigma_\infty c|_{x=\varepsilon} + \dfrac{D_0}{u_s} g_l(x - \varepsilon), \\[2mm] c_l = 1 + c_1\left[1 + (G_l(x - \varepsilon) - c|_{x=\varepsilon})\dfrac{\partial D}{\partial \theta} m\sigma_\infty / D_0\right]^{-p}, \quad p = \dfrac{D_0 + \beta_1 m\sigma_\infty D_T G_l}{m\sigma_\infty(\partial D / \partial \theta)G_l}. \end{array}\right\} \tag{16}$$

Here $c|_{x=0}$ and $c|_{x=\varepsilon}$ denote the dimensionless concentrations at the boundaries $x = 0$ and $x = \varepsilon$, and c_1 is a constant of integration; all of them are determined below.

Integration of equation (13) gives

$$\frac{dc}{dx} = -\frac{\varphi(x) + c_2}{N\Lambda(\varphi)}, \tag{17}$$

where c_2 is a constant. Substituting $\mathrm{d}c/\mathrm{d}x$ from (17) in (12) and multiplying the result by $\mathrm{d}x/\mathrm{d}\varphi$, we arrive at the following equation:

$$\frac{\mathrm{d}}{\mathrm{d}\varphi}\left[(1-\varphi)c - (1-\varphi)(a-bc)\frac{\varphi+c_2}{N\Lambda(\varphi)}\right] + kc = 0.$$

Now, it is easy to see that the dimensionless concentration c depends only on φ (a similar result was obtained earlier for linear diffusion transport by Alexandrov 2001). Integration of the above equation gives

$$c(\varphi) = F(\varphi)(c|_{x=\varepsilon} + J(\varphi)), \tag{18}$$

where

$$F(\varphi) = \frac{\lambda_s}{\lambda_l}\Lambda(\varphi)\left(1-\frac{1}{q}\varphi\right)^{\alpha}(1-\varphi)^{\beta}, \quad J(\varphi) = -\int_0^\varphi \frac{1}{F(x)}\frac{h_1(x)}{h_2(x)}\,\mathrm{d}x,$$

$$h_1(x) = a\frac{x+c_2}{N\Lambda(x)} - a(1-x)\frac{\mathrm{d}}{\mathrm{d}x}\left(\frac{x+c_2}{N\Lambda(x)}\right), \quad h_2(x) = (1-x)\left(1+b\frac{x+c_2}{N\Lambda(x)}\right),$$

$$r = -\left(1-\frac{\lambda_l}{\lambda_s}\right)N - b, \quad q = \frac{1}{r}\left(\frac{\lambda_l}{\lambda_s}N + bc_2\right),$$

$$\alpha = \frac{\gamma_1 + \gamma_2 q}{r(1-q)} - 1, \quad \beta = -\frac{\gamma_1 + \gamma_2}{r(1-q)},$$

$$\gamma_1 = (k-1)\frac{\lambda_l}{\lambda_s}N - bc_2, \quad \gamma_2 = (k-1)\left(1-\frac{\lambda_l}{\lambda_s}\right)N - b.$$

Further, combining expressions (14), (15) and (17), we have

$$u_s = \frac{\lambda_s g_s - \lambda_l g_l}{L_V}, \quad c_2 = \frac{\lambda_l g_l}{\lambda_s g_s - \lambda_l g_l}. \tag{19}$$

It is easily seen that the rate of solidification is the same as for the planar front. Thus, the nonlinear solute transport under consideration does not produce any changes in the rate of solidification.

The value of c_1 is found from equations (15):

$$c_1 = \frac{G_l}{1+\beta_1 m\sigma_\infty D_T G_l/D_0}\left[1-c|_{x=\varepsilon}\frac{\partial D}{\partial\theta}m\sigma_\infty/D_0\right]^{p_1}, \quad p_1 = \frac{1+bG_l}{m\sigma_\infty(\partial D/\partial\theta)G_l/D_0}.$$

Combining conditions (15) and (16), we find the impurity concentration at the boundary $x = \varepsilon$:

$$c|_{x=\varepsilon} = \frac{1 + (1 + \beta_1 m\sigma_\infty D_T/D_0)\,G_l}{1 + bG_l}. \tag{20}$$

To find the bulk fraction φ_* at the left boundary $x = 0$, we substitute $\mathrm{d}c/\mathrm{d}x$ from (17) and $c(\varphi_*)$ from (18) in the second boundary condition (14). This gives the following algebraic equation for φ_*:

$$F(\varphi_*)(c|_{x=\varepsilon} + J(\varphi_*)) = \frac{a}{b + (1-k)N\Lambda(\varphi_*)/(\varphi_* + c_2)}. \tag{21}$$

It is easy to see that the bulk fraction φ_* is completely determined by physical and operating parameters of the process.

Differentiation of $c(\varphi)$ with respect to x gives

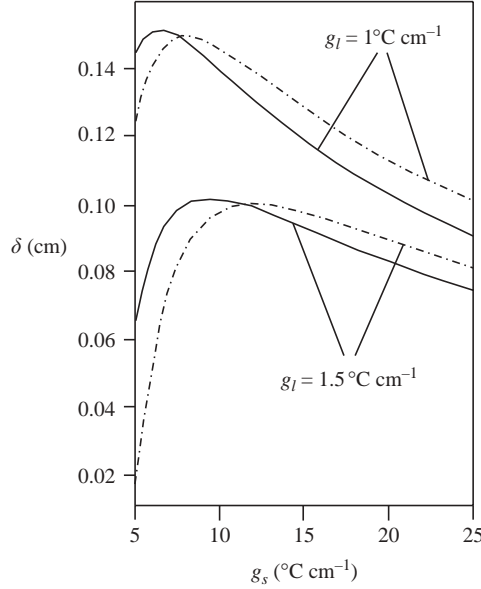$$\frac{\mathrm{d}\varphi}{\mathrm{d}x} = \frac{\mathrm{d}c/\mathrm{d}x}{\mathrm{d}c/\mathrm{d}\varphi}.$$

FIGURE 1. The dimensional mushy zone thickness δ as a function of g_s and g_l for the Fe–Ni alloy, $k = 0.68$, $m = 2.65\,^\circ\text{C(wt\%)}^{-1}$, $L_V = 3398.5\,\text{cal cm}^{-3}$, $D_0 = 5 \times 10^{-5}\,\text{cm}^2\,\text{s}^{-1}$, $\lambda_l = 0.1\,\text{cal}$ $(\text{s cm}\,^\circ\text{C})^{-1}$, $\lambda_s = 0.177\,\text{cal}\,(\text{s cm}\,^\circ\text{C})^{-1}$, $\sigma_\infty = 0.3$, $D_T = 10^{-6}\,\text{cm}^2\,(\text{s}\,^\circ\text{C})^{-1}$, $\partial D/\partial\theta = 10^{-5}\,\text{cm}^2$ $(\text{s}\,^\circ\text{C})^{-1}$. Model II (solid curves) is compared with the classical case (dash-dot curves).

Substituting $\text{d}c/\text{d}x$ and $\text{d}c/\text{d}\varphi$ from equations (17) and (18), and taking into consideration that $\varphi = \varphi_*$ at $x = 0$, we obtain $x(\varphi)$ in the form

$$x(\varphi) = \int_\varphi^{\varphi_*} \frac{\text{d}}{\text{d}z}[F(z)(c|_{x=\varepsilon} + J(z))]\frac{N\Lambda(z)}{z + c_2}\,\text{d}z. \tag{22}$$

If this function is known, it is not difficult to plot the inverse function $\varphi(x)$. Substituting $\varphi = 0$ at $x = \varepsilon$ into expression (22), we find the dimensional two-phase zone thickness $\delta = D_0\varepsilon/u_s$:

$$\delta = \frac{D_0}{u_s}\int_0^{\varphi_*} \frac{\text{d}}{\text{d}z}[F(z)(c|_{x=\varepsilon} + J(z))]\frac{N\Lambda(z)}{z + c_2}\,\text{d}z. \tag{23}$$

Figure 1 illustrates the mushy zone thickness $\delta(g_s)$ for different values of g_l (to demonstrate the behaviour of curves clearly, we used overestimated values of D_T and $\partial D/\partial\theta$; the qualitative behaviour corresponds to typical values used in figures 2 and 3). It is clearly seen that the two-phase zone thickness attains its maximum at a certain temperature gradient (similar behaviour was observed previously by Alexandrov (2001) for the linear form of the diffusion flux). As shown in figure 1, the mushy zone thickness in the classical case (Alexandrov 2001) is less than in the case under study for some values of g_s. Increasing the temperature gradient in the solid changes this behaviour. This appears to be caused by the following processes. The temperature near boundary $x = 0$ is less than the melting temperature of the pure melt (see (5)), so increasing $\partial D/\partial\theta$ decreases the diffusion coefficient (see (2)) and, consequently, decreases the impurity output from the phase transition boundary $x = 0$. Therefore, the concentration of impurity in the classical case is less (greater) than this value in the case under study at $x = 0$ ($x = \varepsilon$). This assists supercooling near the mush/liquid boundary and increasing the mushy zone thickness (see regions in figure 1
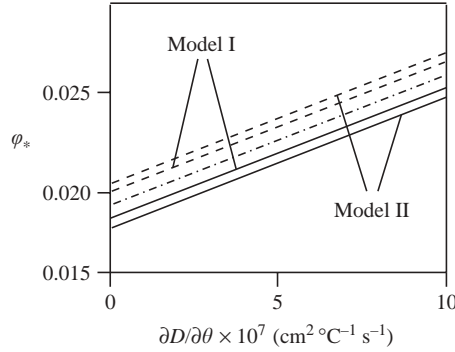
FIGURE 2. The bulk fraction of the solid phase at the solid/mush interface as a function of the temperature coefficient $\partial D/\partial\theta$ for the Fe–Ni alloy, $g_l = 30\,°\text{C}\,\text{cm}^{-1}$ and $g_s = 100\,°\text{C}\,\text{cm}^{-1}$. Solid, dashed and dash-dot curves correspond to $D_T = -12.1 \times 10^{-8}\,\text{cm}^2\,(\text{s}\,°\text{C})^{-1}$, $D_T = 12.1 \times 10^{-8}\,\text{cm}^2\,(\text{s}\,°\text{C})^{-1}$ and $D_T = 0$, respectively.
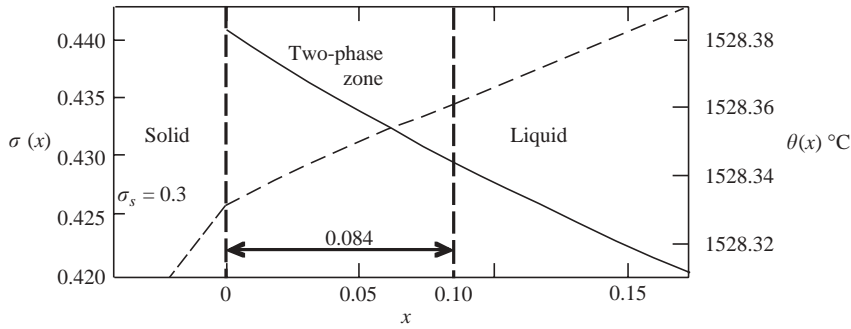

FIGURE 3. The concentration of impurity σ (scale of values on the left, solid curve) and temperature θ (scale of values on the right, dashed curve) as functions of dimensionless spatial coordinate x for the Fe–Ni alloy, $D_T = -12.1 \times 10^{-8}\,\text{cm}^2\,(\text{s}\,°\text{C})^{-1}$ (Kubicek & Mrazek 2001), $\partial D/\partial\theta = 5 \times 10^{-7}\,\text{cm}^2\,(\text{s}\,°\text{C})^{-1}$ (typical value for metallic alloys), $g_l = 30\,°\text{C}\,\text{cm}^{-1}$ and $g_s = 100\,°\text{C}\,\text{cm}^{-1}$ (Model II). σ_s is the impurity concentration in the solid obtained in accordance with the boundary condition $\sigma_s = k\sigma$ at $x = 0$.

on the right of the intersection points of solid and dashed-dot curves). However, the impurity transported from the solid/mush interface at small temperature gradients g_s is weakly cooled. In other words, the mushy zone thickness is determined in the first place by supercooling near boundary $x = 0$. Since the impurity concentration in the case of Model II is greater than in the classical case, the mushy zone width is also greater (see regions in figure 1 on the left of the intersection points of solid and dashed-dot curves).

Figure 2 demonstrates the bulk fraction of the solid as a function of nonlinear transport coefficients $\partial D/\partial\theta$ and D_T. Our calculations show that changes (distances between the dash-dot and other curves in figure 2 at fixed values of $\partial D/\partial\theta$) caused only by the Soret effect are of the order of 5% in comparison with the classical case $D_T = 0$. Taking into account possible variations in the temperature coefficient, we conclude that changes attain 25%. In addition, figure 2 shows that positive/negative values of D_T increase/decrease the fraction of φ_*. To gain greater insight into why the above statement is valid, let us consider to figure 3 and expression (1). Figure 3 shows that the impurity concentration σ decreases and the temperature θ increases

with the spatial coordinate. This means that their gradients are negative and positive respectively. In the case of $D_T < 0$, the mass fluxes caused by the Soret effect and normal diffusion are in one direction (see (1)), that is the mass output from the two-phase zone becomes greater. This increases the temperature and decreases the bulk fraction φ_*. In the case of $D_T > 0$, the two fluxes act in opposite directions and, as a consequence, the thermodiffusion assists the growth of the bulk fraction.

Note that the temperature in the mushy zone is also known (see (5)). Thus, the steady-state solidification with thermodiffusion and temperature-dependent diffusivity in the mushy zone is studied analytically. All characteristics of the process under consideration obtained using expressions (16), (18), (22), (23) are plotted in figure 3.

4. Replacement of a mushy zone by a discontinuity surface

The solidification regime with a two-phase zone may be unstable to small morphological and dynamical perturbations (Anderson & Worster 1995, 1996; Alexandrov 2000). If this is the case, it is necessary to carry out an instability analysis of the above solutions. This procedure is well-detailed for frontal models (Mullins & Sekerka 1964; Wollkind & Segel 1970; Alexandrov 2004 for linear and Van Vaerenbergh *et al.* 1995, 1996, 2001 for nonlinear mass transfer). Therefore, let us consider a new model of solidification with a quasi-equilibrium mushy zone. The key idea of this model is to replace a mushy zone by a discontinuity surface between the solid and liquid phases. The validity of such a replacement follows from the fact that the two-phase zone width, as a rule, is much smaller than the domain of solidification. Distributions (20) and (21) make it possible to calculate the step changes in thermodynamic quantities and fluxes upon transition through the mushy region and to thus obtain a new formulation of the problem of solidification with such a region.

Replacing the two-phase zone by the discontinuity surface ('front') $\xi = \Sigma(\tau)$, we have the equations of heat and mass transfer in the liquid and solid:

$$\frac{d^2\theta_l}{d\xi^2} = 0, \quad \frac{\partial \sigma_l}{\partial \tau} = -\frac{\partial}{\partial \xi} J_l, \quad \xi > \Sigma(\tau), \tag{24}$$

$$\frac{d^2\theta_s}{d\xi^2} = 0, \quad \xi < \Sigma(\tau). \tag{25}$$

These differential equations of the second kind include unknown functions $\theta_l = \theta_l(\xi, \tau), \theta_s = \theta_s(\xi, \tau), \sigma_l = \sigma_l(\xi, \tau)$. The discontinuity surface coordinate $\Sigma(\tau)$ is unknown too because this coordinate may be dependent on small morphological perturbations arising from, for example, oscillations in the constitutional supercooling. In order that the new model be correct seven boundary conditions are required, three of which are conditions far from the 'front' (so, for example, temperature gradients and solute concentration may by regarded as given far from the discontinuity surface).

Let us find the rest boundary conditions at the 'front'. First, the temperature at the mush/liqid boundary is equal to the phase transition temperature

$$\theta_l = \theta_0 - m\sigma_l, \quad \xi = \Sigma(\tau). \tag{26}$$

Second, taking into consideration that $\theta = \theta_0 - m\sigma$ (or $\partial\theta/\partial\xi = -m\partial\sigma/\partial\xi$) within the mushy zone and $\partial\theta/\partial\xi = \partial\theta_l/\partial\xi, \partial\sigma/\partial\xi = \partial\sigma_l/\partial\xi$ at the mush/liquid boundary, we obtain the condition

$$\frac{\partial\theta_l}{\partial\xi} = -m\frac{\partial\sigma_l}{\partial\xi}, \quad \xi = \Sigma(\tau). \tag{27}$$

Third, replacing u_s by $d\Sigma/d\tau$, g_l by $d\theta_l/d\xi$ and g_s by $d\theta_s/d\xi$, in accordance with expression (19), we obtain

$$\lambda_s \frac{d\theta_s}{d\xi} - \lambda_l \frac{d\theta_l}{d\xi} = L_V \frac{d\Sigma}{d\tau}, \quad \xi = \Sigma(\tau). \tag{28}$$

Let us now deduce the last boundary condition at the discontinuity surface. For this purpose, we calculate the jump in the solute concentration at $\xi = \Sigma(\tau)$ by means of expressions (20) and (21):

$$m\sigma_\infty(c|_{x=\varepsilon} - c|_{x=0}) = \theta_s - \theta_l$$
$$= m\sigma_\infty \left(1 + \frac{(1 - m\sigma_\infty(\partial D/\partial \theta)/D_0)G_l}{1 + bG_l} - \frac{a(\varphi_* + c_2)/(N\Lambda(\varphi_*))}{1 - k + b(\varphi_* + c_2)/(N\Lambda(\varphi_*))} \right). \tag{29}$$

The jump in derivatives at the discontinuity surface is

$$\left. \frac{dc}{dx} \right|_{x=0} - \left. \frac{dc}{dx} \right|_{x=\varepsilon} = \frac{1}{m\sigma_\infty} \left[\frac{d\theta_l}{dx} - \frac{d\theta_s}{dx} \right] = G_l - \frac{\varphi_* + c_2}{N\Lambda(\varphi_*)}.$$

We take the magnitude of $(\varphi_* + c_2)/(N\Lambda(\varphi_*))$ from the last equation, and substitute the result in (29). Replacing g_l by $d\theta_l/d\xi$, g_s by $d\theta_s/d\xi$, d/dx by $u_s^{-1}D_0 d/d\xi$ and u_s by $d\Sigma/d\tau$ again, we finally obtain

$$\theta_s - \theta_l - m\sigma_\infty = \frac{(D_0 - m\sigma_\infty \partial D/\partial \theta)\, \partial\theta_l/\partial\xi}{d\Sigma/d\tau + (\partial D/\partial\theta + \beta_1 D_T)\, \partial\theta_l/\partial\xi}$$
$$- \frac{(D_0 - \beta_0 m D_T)\partial\theta_s/\partial\xi}{(1-k)\, d\Sigma/d\tau - (\partial D/\partial\theta + \beta_1 D_T)\, \partial\theta_s/\partial\xi}, \quad \xi = \Sigma(\tau). \tag{30}$$

This boundary condition and the above model are identical to the conditions obtained by Alexandrov (2001) in the classical case: $\partial D/\partial\theta = 0$, $\beta_0 = 0$ and $\beta_1 = 0$. Thus, the frontal model (24)–(28), (30) describing directional solidification with a mushy zone is derived. This model allows an instability analysis to be carried out in the spirit of Van Vaerenbergh *et al.* (1995, 1996, 2001).

5. Conclusion

Exact analytical solutions of the nonlinear model (1)–(11) describing directional crystallization have been obtained. The thermodiffusion and temperature-dependent diffusivity modifying the heat and mass transfer during the solidification were found to be significant. The model under consideration demonstrates a complex behaviour of the mushy zone thickness dependent on the temperature gradients and variations in the diffusion coefficient (figure 1). The influence of the Soret effect on the crystallization process is characterized by the sign of the thermodiffusion coefficient (figure 2). Thus, the solidification under study is completely described by the analytical expressions (16), (18)–(23), on the basis of which the new 'frontal' model of a mushy zone is derived.

REFERENCES

ALEXANDROV, D. V. 2000 Linear analisis of dinamic instability of solidification with a quasiequilibrium mushy zone. *Intl J. Fluid Mech. Res.* **27**, 239–247.

ALEXANDROV, D. V. 2001 Solidification with a quasiequilibrium mushy region: analytical solution of nonlinear model. *J. Cryst. Growth* **222**, 816–821.

ALEXANDROV, D. V. 2004 A nonlinear instability analysis of crystallization processes with a two-phase zone. *J. Metastable Nanocrystalline Mater.* **20–21**, 468–475.

ANDERSON, D. & WORSTER M. G. 1995 Weakly-nonlinear analisis of convection in a mushy layer during the solidification of binary alloy. *J. Fluid Mech.* **302**, 307–331.

ANDERSON, D. & WORSTER M. G. 1996 A new oscillatory instability in a mushy layer during the solidification of binary alloy. *J. Fluid Mech.* **307**, 245–267.

BATCHELOR, G. K. 1974 Transport properties of two-phase materials with random structure. *Annu. Rev. Fluid Mech.* **6**, 227–255.

BORISOV, V. T. 1987 *Theory of Two-phase (mushy) Zone of a Metal Ingot.* Metallurgiya Publishing House, Moscow.

BRUSON, A. & GERL, M. 1980 Diffusion coefficient of Sn, Sb, Ag and Au in liquid Sn. *Phys. Rev.* B **21**, 5447–5454.

BUYEVICH, YU. A., ALEXANDROV, D. V. & MANSUROV, V. V. 2001 *Macrokinetics of Crystallization.* Begell House, New-York-Wallingford.

FOWLER, A. C. 1985 The formation of freckles in binary alloys. *IMA J. Appl. Maths* **35**, 159–174.

HILLS, R. N., LOPER, D. E. & ROBERTS, P. H. 1983 A thermodynamically consistent model of a mushy zone. *Q. J. Mech. Appl. Math.* **36**, 505–539.

HOLLINGER, ST. & LÜCKE, M. 1995 Influence of the Dufour effect on convection in binary gas mixtures. *Phys. Rev.* E **52**, 642–657.

HUPPERT, E. H. & WORSTER, M. G. 1985 Dynamic solidification of a binary melt. *Nature* **314**, 703–707.

IVANTSOV, G. P. 1951 The diffusion supercooling in crystallization of a binary mixture. *Dokl. Akad. Nauk SSSR* **81**, 179–182.

KERR, R. C., WOODS, A. W., WORSTER, M. G. & HUPPERT, H. E. 1990*a* Solidification of an alloy cooled from above. Part 1. Equilibrium growth. *J. Fluid Mech.* **216**, 323–342.

KERR, R. C., WOODS, A. W., WORSTER, M. G. & HUPPERT, H. E. 1990*b* Solidification of an alloy cooled from above. Part 2. Non-equilibrium interfacial kinetics. *J. Fluid Mech.* **217**, 331–348.

KERR, R. C., WOODS, A. W., WORSTER, M. G. & HUPPERT, H. E. 1990*c* Solidification of an alloy cooled from above. Part 3. Compositional stratification within the solid. *J. Fluid Mech.* **218**, 337–354.

KUBICEK, P. & MRAZEK, L. 2001 Thermodiffusion and vaporization of metall from levitated droplet V. *Czech. J. Phys.* **46**, 567–580.

MULLINS, W. W. & SEKERKA, R. F. 1964 Stability of a planar interface during solidification of a dilute binary alloy. *J. Appl. Phys.* **35**, 444–451.

PRAIZEY, J. P. 1989 Benefits of microgravity for measuring thermotransport coefficients in liquid metallic alloys *Intl J. Heat Mass Transfer* **32**, 2385–2401.

VAN VAERENBERGH, S., CORIELL, S. R. & MCFADDEN, G. B. 2001 Morphological stability of a binary alloy: thermodiffusion and temperature-dependent diffusivity. *J. Cryst. Growth* **223**, 565–572.

VAN VAERENBERGH, S., CORIELL, S. R., MCFADDEN G. B., MURRAY B. T. & LEGROS, J. C. 1995 Modification of morphological stability by Soret diffusion. *J. Cryst. Growth* **147**, 207–214.

VAN VAERENBERGH, S., GARANDET, J. P., PRAIZEY J. P. & LEGROS, J. C. 1998 Reference Soret coefficients of natural isotopes and diluted alloys of tin. *Phys. Rev.* E **58**, 1866–1873.

VAN VAERENBERGH, S., LEGROS, J. C. & HENNENBERG, M. 1996 Oscillations induced by purely diffusive processes in planar directional solidification from the melt. *J. Cryst. Growth* **158**, 369–376.

WOLLKIND, D. J. & SEGEL, L. A. 1970 A nonlinear stability analisis of the freezing of a dilute binary alloy. *Phil. Trans. R. Soc. Lond.* A **268**, 351–380.

WORSTER, M. G. 1986 Solidification of an alloy from a cooled boundary. *J. Fluid Mech.* **167**, 481–501.